

Application of dose-gradient function in reducing radiation induced lung injury in breast cancer radiotherapy

Han Bai^{a,b,1}, Hui Song^{a,1}, Qianyan Li^{a,1}, Jie Bai^c, Ru Wang^a, Xuhong Liu^a,
Feihu Chen^a and Xiang Pan^{a,*}

^a*Department of Radiation Oncology, Yunnan Cancer Hospital, The Third Affiliated Hospital of Kunming Medical University, Cancer Center of Yunnan Province, Xishan District, Kunming, Yunnan, People's Republic of China*

^b*Department of Physics and Astronomy, Yunnan University, Kunming, Yunnan*

^c*Department of Radiation Oncology, Daqin Tumor Hospital, Guiyang, Guizhou, China*

Received 4 August 2023

Revised 19 October 2023

Accepted 20 October 2023

Abstract.

OBJECTIVE: Try to create a dose gradient function (DGF) and test its effectiveness in reducing radiation induced lung injury in breast cancer radiotherapy.

MATERIALS AND METHODS: Radiotherapy plans of 30 patients after breast-conserving surgery were included in the study. The dose gradient function was defined as $DGF = \sqrt[3]{\frac{V_D}{V_P}}$, then the area under the DGF curve of each plan was calculated in rectangular coordinate system, and the minimum area was used as the trigger factor, and other plans were triggered to optimize for area reduction. The dosimetric parameters of target area and organs at risk in 30 cases before and after re-optimization were compared.

RESULTS: On the premise of ensuring that the target dose met the clinical requirements, the trigger factor obtained based on DGF could further reduce the V_5 , V_{10} , V_{20} , V_{30} and mean lung dose (MLD) of the ipsilateral lung in breast cancer radiotherapy, $P < 0.01$. And the D_{2cc} and mean heart dose (MHD) of the heart were also reduced, $P < 0.01$. Besides, the NTCPs of the ipsilateral lung and the heart were also reduced, $P < 0.01$.

CONCLUSION: The trigger factor obtained based on DGF is efficient in reducing radiation induced lung injury in breast cancer radiotherapy.

Keywords: Radiation induced lung injury, dose gradient function, trigger factor, re-optimization, breast-conserving surgery

¹These authors contributed equally to this study and share first authorship.

*Corresponding author: Xiang Pan, Department of Radiation Oncology, Yunnan Cancer Hospital, The Third Affiliated Hospital of Kunming Medical University, Cancer Center of Yunnan Province, No. 519 Kunzhou Road, Xishan District, Kunming, 650118, Yunnan, People's Republic of China. E-mail: pxiangnn@163.com.

1. Introduction

Radiotherapy is the most important treatment for breast cancer after breast-conserving surgery, which has significant value in reducing the local recurrence rate and clinical mortality. Many studies have shown that volumetric modulated arc therapy (VMAT) is widely used in breast cancer after breast-conserving surgery, which can increase the target dose, improve the target dose distribution, significantly shorten the treatment time and reduce the dose of normal tissues [1–5].

Chest wall irradiation can affect the lung by exposing some of them to the radial and do harm to them, resulting various degrees of radiation-induced lung injury. In the era of three-dimensional radiotherapy, V_{20} , V_5 and mean dose of lung are commonly used to predict radiation-induced pneumonitis [6–9]. A prospective study [10] found that the volume of lung irradiated was closely related to the occurrence of radiation-induced lung injury, and was significantly related to the severity of radiation-induced lung injury. When $V_{20} \leq 20\%$, no radiation-induced lung injury occurred. Only 8% of the patients had radiation-induced lung injury when V_{20} is equal to 22%–31%, and no grade 3 radiation-induced lung injury occurred. Lind et al [11]. found that ipsilateral lung $V_{20} < 30\%$ could significantly reduce the incidence of radiation pneumonitis in postoperative radiotherapy for breast cancer. Zeng Yuanyuan et al [12]. found that the incidence of radiation-induced lung injury after radical mastectomy was 9.78%, and most of them were grade 1 injury. The lung volume ratio receiving more than 20Gy (V_{20}) was an independent risk factor for radiation-induced lung injury after radical mastectomy. The V_{20} value can be used to predict and recommend radiotherapy, which can effectively reduce the incidence of radiation injury. Therefore, the irradiated volume and dose of the lung should be carefully evaluated to minimize the irradiation to the normal lung tissue before radiotherapy.

Doctors and physicists still rely on dose volume histogram (DVH) and traditional layer-by-layer visualization of isodose lines to evaluate plans. It is difficult for doctors to choose different plans that can generate almost the same dose distribution. Physicists are puzzled by how to quantitatively determine whether a parameter in a plan has the space for decline. In order to fully evaluate the quality of the plan, in addition to the commonly used indicators of conformity such as conformity index (CI) and heterogeneity index (HI), it is also necessary to evaluate the dose gradient to ensure an optimal dose attenuation around the target. Some studies [13–16] have introduced different gradient indices to achieve the degree of dose attenuation near the target. Sung et al. [17] proposed a new dose gradient curve (DGC) suitable for clinical practice, and they believed that DGC was a reasonable method to visualize the dose gradient as the average distance between two isodose planes. The shorter the distance, the steeper the dose gradient. In this study, a dose gradient function (DGF) was defined and a dose gradient evaluation tool based on the relative spatial relationship between isodose lines was introduced, in order to provide a basis for physicists to evaluate and further optimize the plan.

2. Materials and methods

2.1. Patient selection

Thirty patients who had received with Volumetric Modulated Arc Radiotherapy (VMAT) for left breast cancer after breast-conserving surgery were included in this retrospective study. Requirements on cases selection were as follows: enough exercises were carried out on the same side upper limb to meet requirements of body posture in CT localization and treatment; No lymph node metastasis; KPS > 90. The mean age of the study group was 49 (range from 32 to 65). The range of planned target volume (PTV) was from 354.32 to 1615.03 cm³.

Table 1
The optimization constraints of plans

PTV/OARs	Constraint conditions	Objectives
PTV	D_{99}	≥ 50 Gy
	D_{max}	≤ 55 Gy
L-lung	V_{20}	$< 30\%$
R-lung	V_{20}	$< 10\%$
Heart	D_{mean}	< 4 Gy
C-Breast	D_{mean}	< 6 Gy
Cord	D_{max}	< 30 Gy

2.2. Target region delineation

After computed tomography (CT) simulation, the scanned image was sent to the Monaco treatment planning system (TPS, Version: 5.40.03). Organs at risk (heart, left and right lungs, spinal cord, contralateral breast) were segmented; target region clinical target volume (CTV) was segmented by the clinician. On the basis of CTV, the inside, outside, and back limits were extended 5 mm, respectively, to generated PTV, with the boundary under skin.

2.3. Planning formulation

All plans adopted 6-MV X-ray and Elekta VERSA HD accelerator (Stockholm, Sweden, 5 mm MLC), with prescription doses all set to 2.0Gy * 25 fractions. Monaco TPS (Elekta. Inc, V 5.40.03). was adopted for plan optimization, which utilized Monte Carlo for the dose calculation 1 arc, 150~260 degree was designed, and according to the shape of target region, corresponding collimator angles were set, table angles all 0°, maximum dose rate 600 MU/min. After providing some optimizing constraints (shown in Table 1), distribution of dose curves was automatically optimized, and through repeated parameters adjustment, the ideal distribution of dose curves was achieved.

2.4. The definition of dose gradient function (DGF)

VMAT is a multi-field focused radiotherapy technique, which forms the distribution characteristics of isodose lines decreasing outward from the target area. The rate at which the radiation dose decreases outward from the target area determines the range of radiation dose received by the surrounding normal tissues. The faster decay rate, the less normal tissues are irradiated around the target area, and the higher the quality of the radiotherapy plan. In this study, dose gradient function (DGF) was defined and utilized to quantify the decay rate of dose and to guide the re-optimization of the plan, improving the quality of the radiotherapy plan. The DGF was defined as follows:

$$DGF = \sqrt[3]{\frac{V_D}{V_P}} \quad (1)$$

where V_D is the volume of isodose line generated structure, V_P is the volume of target (PTV). According to the above definition DGF, the thirty VMAT plans were analyzed. The volume of isodose line (from V_{50Gy} to V_{15Gy} , the step size is 0.25Gy) was generated for each case, and then the DGF was calculated. The Dose-DGF curve was plotted as shown in Fig. 1.

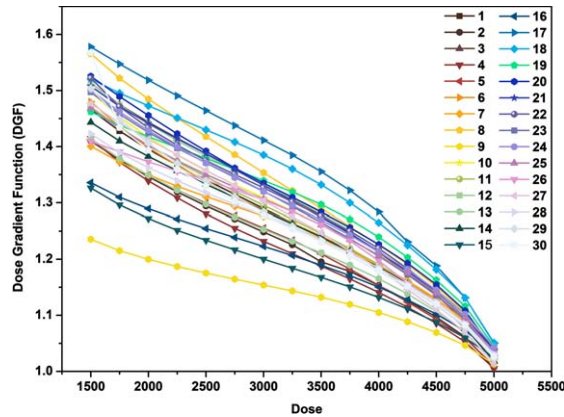


Fig. 1. The Dose-DGF curves of 30 patients.

2.5. The mechanism of DGF guiding radiotherapy plan optimization

2.5.1. A simple example describes the properties of DGF

Figure 2 A, B shows two typical DGF examples, indicating the area where the iso-dose line of 5000cGy-1500cGy intersects the left lung. The shorter the distance between the dose lines, the steeper the dose gradient and the faster the dose attenuation, the smaller the volume of the left lung that receives the radiation dose (Fig. 2A). Meanwhile, according to the formula (1), the lower the value of V_D , the less DGF, therefore, the faster the dose attenuation. As shown in Fig. 2C, the smaller the area under the D-DGF curve, the lower the irradiation dose received by organ at risk (OARs, when $S_{PA} < S_{PB}$, we have $D_{PA,OARs} < D_{PB,OARs}$, here S_{PA} , S_{PB} were indicated as area under the patient's A and B D-DGF curve, D_{PA} ; D_{PA} , D_{PB} were indicated as the dose of patient A and B). Thus, in this study, the area under the D-DGF curve was used as a trigger factor to guide the optimization of the plan, reducing radiation-induced lung injury in breast cancer postoperative radiotherapy.

2.5.2. The mechanism of DGF guiding radiotherapy plan optimization

The area under the D-DGF curve of thirty patients were calculated by GraphPad Prism Software (Table 2). The volume of 2000cGy dose line (V_{20}) of left lung in original plan was statistical. As shown in Table 2, the plan of 9th patient was considered to be the optimal plan, therefore, select and use the minimum area value (S_{min}) as the trigger operator to trigger the re-optimization of other patient plans respectively. The plans were triggered to optimize for area reduction.

2.6. Evaluation parameters

On the premise of meeting clinical requirements, the following comparisons among the plans of before and after optimization were conducted using dose-volume histogram (DVH): V_{95} , V_{100} , V_{107} , V_{110} , D_{98} , and D_2 , as well as conformity and homogeneity of target; mean dose, V_5 , V_{10} , V_{20} , and V_{30} of L-lung; V_5 , V_{10} , V_{20} and mean dose of right lung; D_2 and mean dose of heart; D_1 and mean dose of contralateral breast; maximum dose of the spinal cord; low dose bath (10% Rx); Monitor Unit (MUs). Among statistical indexes of the target region, V_X represents the target volume wrapped by X% prescription dose. In this research, volume parameters were adopted to evaluate minimum and maximum dose in the target region. The minimum dose is that 98% PTV exceeds (D_{98}), and the maximum dose is that 2% PTV exceeds (D_2).

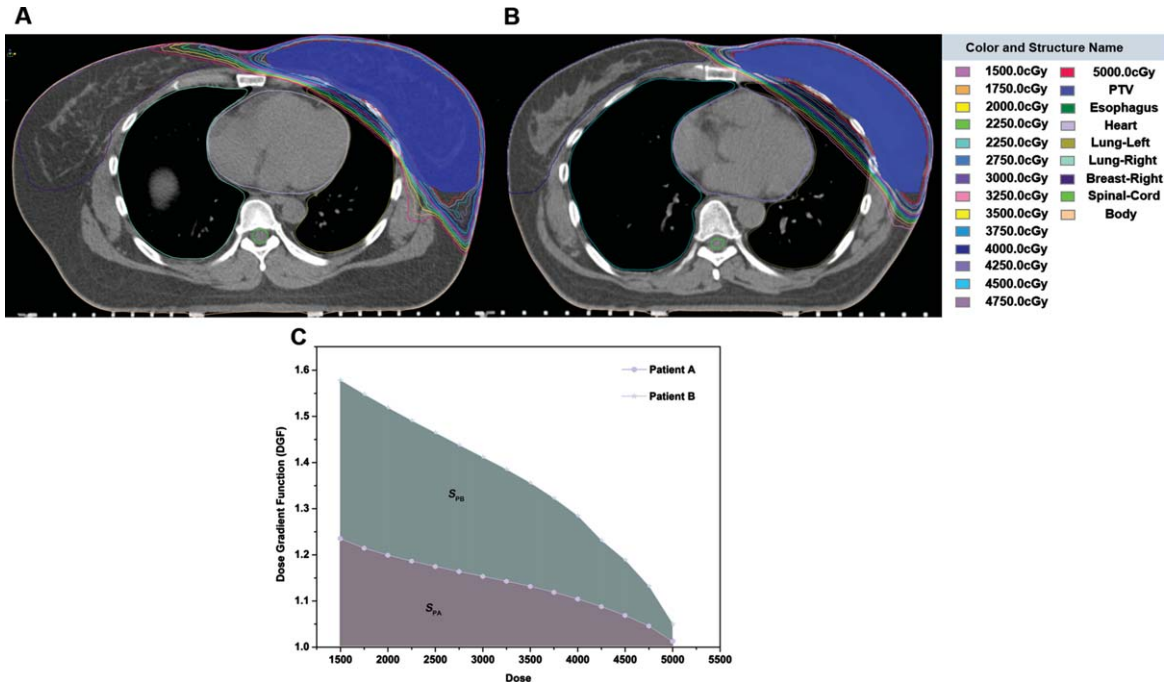


Fig. 2. A, B) Two typical DGF examples; C) The area under the D-DGF curve of representative patient A and B.

Table 2
The area under the D-DGF curve and the V20 of left lung of thirty patients

No	Area (S, cm ²)	V ₂₀ (%)	No	Area (S, cm ²)	V ₂₀ (%)	No	Area (S, cm ²)	V ₂₀ (%)
1	4413	15.6	11	4426	14.8	21	4533	12.26
2	4276	14.5	12	4538	18.4	22	4524	12.78
3	4532	13.4	13	4300	11.4	23	4496	9.76
4	4238	11.6	14	4390	11.9	24	4512	13.47
5	4287	11.9	15	4135	11.9	25	4461	15.48
6	4421	17.2	16	4198	11	26	4413	13.18
7	4355	16	17	4770	22.78	27	4432	20.31
8	4615	17.3	18	4681	20.21	28	4365	10.32
9	3981	10.5	19	4549	17.58	29	4412	5.65
10	4481	11.4	20	4567	15.44	30	4405	20.47

* NO is the number of 30 patients.

2.7. Calculation of radiobiological parameters

According to the Lyman-Kutcher-Burman model, NTCP for V_x of an OAR is given by [18]:

$$NTCP = \frac{1}{\sqrt{2\pi}} \int_{-\infty}^t e^{-\frac{x^2}{2}} dx \tag{2}$$

Where,

$$t = \frac{V_{20} - V_{20,50}}{m \cdot V_{20,50}} \tag{3}$$

Table 3
Comparison of tumor target dose between the original plan and the DGF plan in 30 patients

Evaluation parameters	Original plan	DGF plan	<i>P</i> value
V_{95} (%)	98.91 ± 0.75	98.69 ± 0.50	0.133
V_{100} (%)	95.26 ± 0.56	95.31 ± 0.61	0.332
V_{107} (%)	11.25 ± 18.14	6.26 ± 6.73	0.190
V_{110} (%)	2.24 ± 6.94	0.65 ± 1.20	0.236
D_2 (cGy)	5408.03 ± 87.22	5393.48 ± 72.07	0.527
D_{98} (cGy)	4848.89 ± 100.85	4853.85 ± 59.84	0.806
10% Rx (cm ³)	3809.34 ± 120.34	3656.69 ± 121.23	0.25
MUs	897.94 ± 130.18	935.57 ± 114.11	0.134

Where, V_{20} represents the volume of the OAR receiving the dose of ≥ 20 Gy, and $V_{20, 50}$ represents the volume received under ≥ 20 Gy when the probability of radiotherapy complications is 50%.

In addition, according to literature [19] research results, the probability of radioactive cardiac events will increase by 7.4% when the average cardiac dose increases by 1Gy, that is:

$$\Delta NTCP_{cardiac} = \frac{\Delta MHD(cGy)}{100cGy} \times 7.4\% \quad (4)$$

In this paper, our team selected formulas (2) and (4) to calculate the NTCP of the L- Lung and heart respectively.

2.8. Statistical analysis

The Paired-Samples *T*-test was used to carry out statistical analysis using SPSS statistical software (V.28.0.1, SPSS, Inc., Chicago, IL), and $P < 0.05$ was considered statistically significant.

3. Results

3.1. Comparison of target dose

As shown in Table 3, the radiotherapy plans before and after optimization were compared, the evaluation parameters of PTV were not statistically significant ($P > 0.05$), suggesting that the re-optimization of the plan had no effect on the coverage of the target. Low dose bath (the volume of 500 cGy) and Monitor Unit (MUs) were no statistically significant ($P > 0.05$).

3.2. Comparison of dose parameters of OARs

3.2.1. Left lung

In the radiotherapy of breast cancer, the ipsilateral lung is one of the important OARs. Figure 3 compares of the V_{20} of Left lung between the original plan and the DGF plan in 30 patients, the results showed that after optimization, the V_{20} in the left lung is down (26 of 30 patients). All with statistical significance ($P < 0.001$) observed through paired comparisons (Table 4).

The studies have shown that radiation-induced lung injury after volume-modulated radiotherapy (VMAT) for left breast cancer is correlated with the different dose volumes and mean dose of the ipsilateral lung, and the low dose volume of the ipsilateral lung has a certain degree of influence on the occurrence of radiation-induced lung injury as well as the high dose volume of the ipsilateral

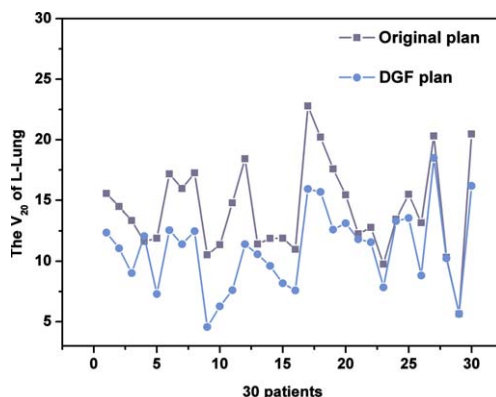


Fig. 3. The V_{20} of Left lung between the original plan and the DGF plan in 30 patients.

Table 4
Comparison of OARs between the original plan and the DGF plan in 30 patients

Evaluation parameters		Original plan	DGF plan	<i>P</i> value
Lung-L	V_5 (%)	43.01 ± 12.67	35.82 ± 7.54	0.005
	V_{10} (%)	25.00 ± 5.74	19.74 ± 4.87	<0.001
	V_{20} (%)	14.28 ± 3.81	10.96 ± 3.30	<0.001
	V_{30} (%)	9.22 ± 3.25	6.45 ± 2.46	<0.001
	MLD (cGy)	920.61 ± 151.73	763.63 ± 143.65	<0.001
Heart	D_{2cc} (cGy)	3261.13 ± 1040.46	2745.45 ± 975.43	0.001
	MHD (cGy)	356.89 ± 69.67	293.84 ± 50.94	<0.001
	Mean (cGy)	1835.32 ± 69.38	1453.06 ± 57.22	<0.01
Lung-R	V_5 (%)	15.11 ± 13.03	9.24 ± 8.84	0.023
	V_{10} (%)	1.90 ± 2.87	0.78 ± 2.15	0.085
	V_{20} (%)	0.04 ± 0.20	0.00 ± 0.01	0.331
	MLD (%)	265.79 ± 128.17	232.56 ± 82.14	0.146
Breast-R	D_{1cc} (cGy)	1782.05 ± 824.25	2026.35 ± 1110.95	0.183
	MBD (cGy)	369.99 ± 159.63	323.19 ± 119.36	0.121
Cord	D_{Max} (cGy)	358.12 ± 230.22	399.45 ± 201.17	0.383

lung. In breast cancer radiotherapy, in addition to paying attention to the traditional predictors of radiation-induced lung injury such as V_{20} , the evaluation of V_5 , V_{10} , V_{30} and MLD should be further strengthened. In this study, we found that when V_{20} decreased, V_5 , V_{10} , V_{30} and MLD also decreased, all with statistical significance ($P < 0.01$) observed through paired comparisons (Table 4). It was concluded that the introduction of DGF could affect the whole dose curve of the left lung.

3.2.2. Other OARs

Comparison of OARs between the original plan and the DGF plan in 30 patients. As shown in Table 4, compared with the original plan, the D_{2cc} and D_{mean} of heart and V_5 of right lung were significantly decreased in the DGF plan guided by dose gradient function, all with statistical significance ($P < 0.05$). In addition, although the V_{10} , V_{20} , D_{mean} of the right lung, D_{1CC} , D_{mean} of the breast-R and D_{Max} were not statistically significant ($P > 0.05$), all met the clinical requirements.

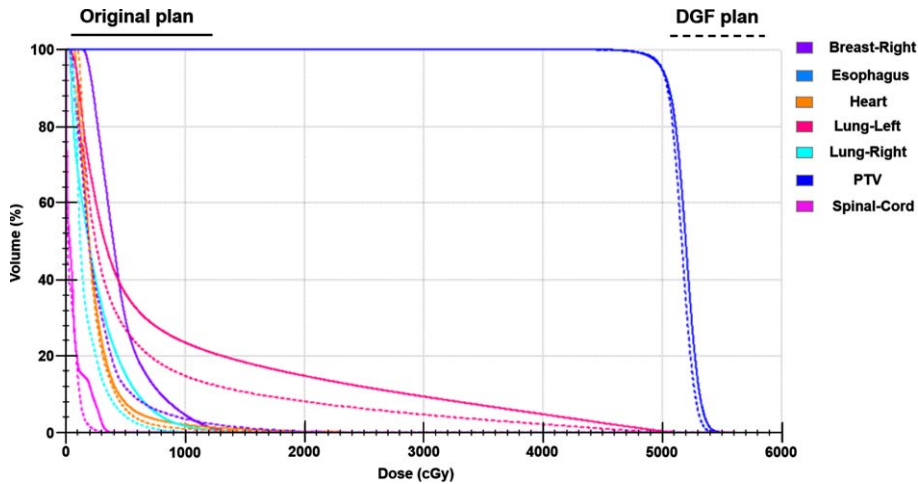


Fig. 4. The DVH curves between the original plan and the DGF plan of the typical patient.

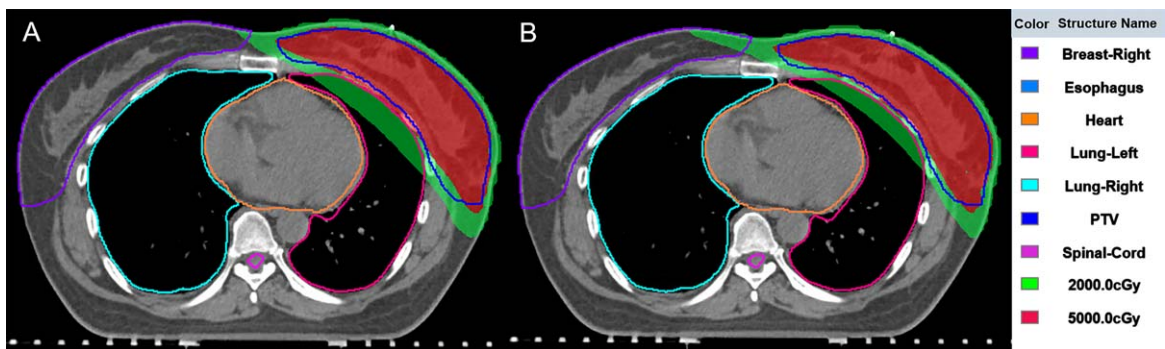


Fig. 5. The dose distribution between the original plan (A) and the DGF plan (B) of the typical patient.

3.3. The DVH and dose distribution of the typical patients

The DVH curves between the original plan and the DGF plan of the typical patient are shown in Fig. 4. The DVH curves illustrate that there was no significant change in the target dose after optimization, however, the doses to OARs were significantly reduced. Figure 5 shows the position relationship between 5000cGy, 2000cGy and the left lung on the patient's transverse section. After optimization (Fig. 5B), the overlap area between 2000cGy and the left lung was smaller, reduces damage to normal left lung tissue.

3.4. Radiobiological results for left lung and heart

The results of NTCP of L-Lung were presented in Table 6, the difference of NTC P value of V_{20} before and after re-optimization was statistically significant ($P < 0.001$). According to the formulas (4), the magnitude of the risk value was calculated and shown in Table 5, the incidence of major coronary decreased from 2.64 % to 2.17% ($P < 0.001$).

Table 5
Comparison of NTCP of left lung and percent increase in rate of major coronary events

Parameters	Type	Original (%)	Re-optimized (%)	t	P
V ₂₀	NTCP	15.00 ± 5.90	10.46 ± 3.94	7.33	<0.001
Heart		2.64 ± 0.51	2.17 ± 0.37	5.73	<0.001

4. Discussions

Breast radiotherapy is challenging and complicated, as the target being located on one side of the body and surrounding organs make this an inherently difficult site to achieve a homogeneous dose distribution. Plane 2D resulted in dose inhomogeneities, particularly in women with larger breasts. An inhomogeneous dose may lead to increased normal tissue side effects and poor cosmetic results, which can cause significant psychological morbidity for patients. The introduction and wide application of CT and computer technology in radiotherapy were the beginning of precise radiotherapy. Three-dimensional conformal radiation therapy (3D-CRT) was the beginning technology of the precise radiotherapy. 3D-CRT followed by Intensity modulated radiation therapy (IMRT), and then many sub-technologies were developed based on IMRT. The study of Selvaraj, et al. showed that the reductions of V₁₀₅ and V₁₁₀ for the IMRT compared to 3DCRT were 44.7% and 66.3%, respectively ($P < 0.01$). The mean dose and V₃₀ for heart with IMRT were 2.3 (SD: 1.1) and 1.05 (SD: 1.5) respectively, which was a reduction by 6.8% and 7.9%, respectively, in comparison with 3D. Similarly, the mean dose and V₂₀ for the ipsilateral lung and the percentage of volume of contralateral volume lung receiving > 5% of prescribed dose with IMRT were reduced by 9.9%, 2.2%, and 35%, respectively [20]. A dosimetric study on radiotherapy for left side breast cancer showed that both VMAT and IMRT led to improved PTV_{95%} coverage (95.63 ± 1.82% in VMAT; 93.70 ± 2.16 % in IMRT; 81.40 ± 6.27% in 3D-CRT) and improved CI (0.96 ± 0.02 in VMAT; 0.91 ± 0.06 in IMRT) as compared to 3D-CRT (0.66 ± 0.11) [21]. It can be seen that the dose of peripheral organs at risk can be reduced effectively by selecting better radiotherapy techniques. But when the technique is not optional, how to judge plans can be improved is remaining a problem.

Therefore, many methods have been raised, which can be used to improve the quality of plans. An earlier model for predicting the dose of OARs in radiotherapy for breast cancer was proposed by Oxford and researchers assessed the value of maximum heart distance (MHD) in predicting the dose and biologically effective dose (BED) to the heart and the left anterior descending (LAD) coronary artery for left-tangential breast or chest wall irradiation [22]. With our proposed DGF optimization, the dose gradient at the edge of the target is improved, the dose “diffused” to the LAD is reduced. And then OVH was proposed, and the OVH achieves a new patient’s DVH by comparing the distance of the OARs and targets of the new patient with those of prior patients, whose plans were maintained in a database. The basis for this calculation was $r_{v,1} \geq r_{v,2} \Rightarrow D_{v,1} \leq D_{v,2}$. For $v > OVH(0)$, we have $r_{v,2} > r_{v,1}$; then $D_{v,2} > D_{v,1}$ was expected. For $v < OVH(0)$, we have $r_{v,1} > r_{v,2}$; then $D_{v,1} < D_{v,2}$ was expected. For $v = OVH(0)$, we have $r_{v,1} = r_{v,2}$; then $D_{v,1} = D_{v,2}$ was expected. This method is effective in predicting the dose of parotid gland in NPC radiotherapy [23]. Several subsequent studies based on OVH expanded the connotation and application scope of OVH [24–26]. However, one shortcoming of these method is that the distance r exists between two points, but the edge of the target is three-dimensional-space curved surface, besides the dose variation occurs in a three-dimensional space. So, only considering the distance in one plane is not enough for optimizing plans.

In the paper, the research team obtained DGF based on the continuance of the dose gradient (DF) concept in SBRT [27–29]. DF’s formula is $DGF = \sqrt[3]{\frac{V_{50\%PD}}{V_p}}$, and the dose “50%PD” is 50% of the

prescribed dose. Because every three-dimensional volume has a sphere that has the same volume. It can be seen that DG reflects the ratio of the radius of the “equivalent sphere” formed by 50% prescription dose in three-dimensional space to the radius of the “equivalent sphere” formed by PTV. In a similar way, DGF’s formula is $DGF = \sqrt[3]{\frac{V_D}{V_P}}$, which reflects the ratio of the radius of the “equivalent sphere” formed by the dose “D” in three-dimensional space to the radius of the “equivalent sphere” formed by PTV. The larger the value of DGF, the larger the ratio and the slower the rate of dose decline. In addition, since the value of DGF varies with D in each physical plan, this study uses the area obtained by integrating DGF to perform its function instead of DGF. When integrating in the same domain ([1500, 5000], as shown in Fig. 2), the smaller the DGF, the smaller the area. The smaller the DGF, the faster the dose decline, i.e., the smaller the dose “diffused” into the ipsilateral lung and heart adjacent to the PTV. This is the reason that when the minimum area triggers plans reoptimize for area reduction, the dose of lung and heart will be reduced, and these results are shown in Table 5 and Fig. 3. Reading Fig. 3 carefully, it is not difficult to find that most plans (26/30) were triggered and re-optimized to achieve lower V_{20} of ipsilateral lung, but some plans (4/30) failed to achieve lower V_{20} . The reason may be that $DGF = \sqrt[3]{\frac{V_D}{V_P}}$ only contains the volume information, but does not contain the shape information of PTV. Experience tells us that the shape of breast cancer PTV, such as the degree of curvature of the PTV, also has some effect on the dose.

The pursuit of lower doses of OARs is essentially an expectation of lower NTCP. So, this study also investigated the change of NTCP caused by the decrease of physical dose, and the results showed that the decrease of physical dose actually resulted in the decrease of NTCP, as shown in Table 6. With the method proposed in this study, the NTCP of the ipsilateral lung can be reduced by about 4.5% and the heart by about 0.5%.

Through the method proposed in this paper, we can review the team’s previous breast-conserving radiotherapy plans to obtain a DGF-curve to guide the design of new plans, or extract a DGF-curve from the plans designed by experienced physicists (dosimetrists) to guide the plan design of entry-level physicists (dosimetrists). Can guarantee continuously improving the quality of plans and keeping the quality level of plans from declining due to the different experiences of the physicist (dosimetrist). In the clinical workflow, the proposed method provides guidance for optimization and, in theory, reduces the number of trial and error in planning. Another potential implication is to programmatically build the recommended methods into TPS to evaluate plans or drive automatic optimization of plans, and our research team will address it in future studies.

5. Conclusion

The dose-gradient function is valid in reducing radiation induced lung injury in breast cancer radiotherapy.

Conflict of interest

The authors declare that the research was conducted in the absence of any commercial or financial relationships that could be construed as a potential conflict of interest.

Author contributions

HB, QL, and XP conceived and designed the study. HS, QL, JB, RW, XL and FC retrieved and analyzed the documents. QL and HS collected the Figures. HB wrote the paper. XP supervised the study, reviewed, and edited the manuscript. All authors approved the final manuscript.

Funding

This work was financially supported by the Science, Technology Department of Yunnan Province (202101AY070001-164).

References

- [1] J.S. Chang, J.H. Chang, N. Kim, K. Kim, et al. Intensity Modulated Radiotherapy and Volumetric Modulated Arc Therapy in the Treatment of Breast Cancer: An Updated Review, *J Breast Cancer* **25**(5) (2022), 349–365.
- [2] H.W. Cheng, C.C. Chang, A.C. Shiau, J.T. Tsai, et al. Dosimetric comparison of helical tomotherapy, volumetric-modulated arc therapy, intensity-modulated radiotherapy, and field-in-field technique for synchronous bilateral breast cancer, *MED DOSIM* **45**(3) (2020), 271–277.
- [3] Y. Yin, J. Chen, T. Sun, R. Wang, et al. Dosimetric research on intensity-modulated arc radiotherapy planning for left breast cancer after breast-preservatxion surgery, *MED DOSIM* **37**(3) (2012), 287–92.
- [4] G.C. Iorio, P. Franco, E. Gallio, U. Ricardi, et al. Volumetric modulated arc therapy (VMAT) to deliver nodal irradiation in breast cancer patients, *MED ONCOL* **35**(1) (2017), 1.
- [5] M. Pasler, J. Lutterbach, M. Björnsgard, D. Georg, et al. VMAT techniques for lymph node-positive left sided breast cancer, *Z MED PHYS* **25**(2) (2015), 104–11.
- [6] L.B. Marks, et al. Dosimetric predictors of radiation-induced lung injury, *Int J Radiat Oncol* **54**(2) (2002), 313–6.
- [7] W.Y. Pan, C. Bian, G.L. Zou, Y.Y. Wang, et al. Combing NLR, V20 and mean lung dose to predict radiation induced lung injury in patients with lung cancer treated with intensity modulated radiation therapy and chemotherapy, *Oncotarget* **8**(46) (2017), 81387–81393.
- [8] J. Chen, J. Hong, X. Zou, W. Zhang, et al. Association between absolute volumes of lung spared from low-dose irradiation and radiation-induced lung injury after intensity-modulated radiotherapy in lung cancer: a retrospective analysis, *J Radiat Res* **56**(6) (2015), 883–8.
- [9] F.H. Zeng and H.T. He, Relationship between radiation-induced lung injury and low-dose irradiated volume in breast cancer patients treated with intensity-modulated radiotherapy, *Chinese Journal of Prescription Drugs* **20**(02) (2020), 165–167.
- [10] M.V. Graham, J.A. Purdy, B. Emami, et al. Clinical dose-volume histogram analysis for pneumonitis after 3D treatment for non-small cell lung cancer (NSCLC), *Int J Radiat Oncol Biol Phys* **45**(2) (1999), 323–329.
- [11] P.A. Lind, L.B. Marks, P.H. Hardenbergh, et al. Technical factors associated with radiation pneumonitis after local+/- regional radiation therapy for breast cancer, *Int J Radiat Oncol* **52**(1) (2002), 137–43.
- [12] Y.Y. Zeng, L. Tao, C. Zhao, Y.F. Deng, et al. Risk Factors of Radiotherapy-induced Lung Injury after Radical Mastectomy, *Chin J Cancer* **35**(04) (2020), 643–646.
- [13] K. Ohtakara, S. Hayashi and H. Hoshi, Dose gradient analyses in Linac-based intracranial stereotactic radiosurgery using Paddick's gradient index: consideration of the optimal method for plan evaluation, *J Radiat Res* **52**(5) (2011), 592–9.
- [14] S. Hossain, P. Xia, K. Huang, L. Ma, et al. Dose gradient near target-normal structure interface for nonisocentric CyberKnife and isocentric intensity-modulated body radiotherapy for prostate cancer, *Int J Radiat Oncol* **78**(1) (2010), 58–63.
- [15] M.K. Giżyńska, P.F. Kukołowicz and P. Kordowski, Implementation of a dose gradient method into optimization of dose distribution in prostate cancer 3D-CRT plans, *Rep Pract Oncol Radi* **19**(6) (2014), 385–91.
- [16] T.A. Reynolds, A.R. Jensen, E.E. Bellairs and M. Ozer, Dose Gradient Index for Stereotactic Radiosurgery/Radiation Therapy, *Int J Radiat Oncol*. **106**(3) (2020), 604–611.
- [17] K. Sung and Y.E. Choi, Dose gradient curve: A new tool for evaluating dose gradient, *PLoS One* **13**(4) (2018), e0196664.
- [18] G.R. Borst, M. Ishikawa, J. Nijkamp, J.J. Sonke, et al. Radiation pneumonitis after hypofractionated radiotherapy: evaluation of the LQ(L) model and different dose parameters, *Int J Radiat Oncol*. **77**(5) (2010), 1596–1603.
- [19] S.C. Darby, M. Ewertz, P. McGale, P. Hall, et al. Risk of ischemic heart disease in women after radiotherapy for breast cancer, *New Engl J Med*. **368**(11) (2013), 987–998.
- [20] R.N. Selvaraj, S. Beriwal, R.J. Pourarian, D.E. Heron, et al. Clinical implementation of tangential field intensity modulated radiation therapy (IMRT) using sliding window technique and dosimetric comparison with 3D conformal therapy (3DCRT) in breast cancer, *MED DOSIM*. **32**(4) (2007), 299–304.
- [21] S.K. Das Majumdar, A. Amritt, S.S. Dhar, D.K. Parida, et al. A Dosimetric Study Comparing 3D-CRT vs. IMRT vs. VMAT in Left-Sided Breast Cancer Patients After Mastectomy at a Tertiary Care Centre in Eastern India, *Cureus* **14**(3) (2022), e23568.

- [22] C.W. Taylor, P. McGale, J.M. Povall, S.C. Darby, et al. Estimating cardiac exposure from breast cancer radiotherapy in clinical practice, *Int J Radiat Oncol.* **73**(4) (2009), 1061–8.
- [23] B. Wu, F. Ricchetti, G. Sanguineti, T. McNutt, et al. Patient geometry-driven information retrieval for IMRT treatment plan quality control, *Med Phys.* **36**(12) (2009), 5497–505.
- [24] Z. Zhou, W. Zhang and S. Guan, An effective calculation method for an overlap volume histogram descriptor and its application in IMRT plan retrieval, *Phys Medica* **32**(10) (2016), 1339–1343.
- [25] B. Wu, D. Pang, S. Lei, S. Collins, et al. Improved robotic stereotactic body radiation therapy plan quality and planning efficacy for organ-confined prostate cancer utilizing overlap-volume histogram-driven planning methodology, *Radiother Oncol* **112**(2) (2014), 221–6.
- [26] B. Wu, D. Pang, P. Simari, T. McNutt, et al. Using overlap volume histogram and IMRT plan data to guide and automate VMAT planning: a head-and-neck case study, *Med Phys* **40**(2) (2013), 021714.
- [27] C.W. Liu, Y.B. Cho, A. Magnelli, et al. The dosimetric impact of titanium implants in spinal SBRT using four commercial treatment planning algorithms, *J Appl Clin Med Phys* (2023), e14070.
- [28] S. Dwivedi, S. Kansal, J. Shukla, et al. Dosimetric assessment of the mono and dual-isocentric VMAT technique based on flattening filter-free beams for SBRT with non-contiguous spinal targets, *Med Dosim.* **48**(2) (2023), 90–97.
- [29] P. Dupuis, M. François, T. Baudier, et al. Evaluation of a dedicated software for semi-automated VMAT planning of spine Stereotactic Body Radiotherapy (SBRT), *Phys Med.* **109** (2023), 102578.